Experimental Validation of Parked Loads for a Floating Vertical Axis Wind Turbine: Wind-Wave Basin Tests

Md Sanower Hossain[1] and D. Todd Griffith[1]

[1]UTD Center for Wind Energy, Department of Mechanical Engineering, University of Texas at Dallas, Richardson, Texas, USA

Correspondence: D. Todd Griffith (tgriffith@utdallas.edu)

Abstract. Parked loads are a major design load case for vertical axis wind turbines (VAWTs) because of persistent high loads on the rotor when in standstill conditions. This paper examines the aerodynamic parked loads of model-scale floating troposkein VAWTs tested in a wind-wave basin to support development and validation of a parked loads model for floating VAWTs. We analyze the effects of wind speed, and turbine solidity (varying number of blades), and rotor azimuth on parked loads and investigate the impact of different wind-wave-platform conditions (comparing locked (fixed tower base) versus floating cases with and without waves). The experimental results indicate that parked loads (for both locked and floating platform conditions) and amplitude of turbine tilting increases with the wind speed, which is expected. The parked loads also increase with the increase of solidity, however the variation in loads in a revolution decreases for 3 blades versus 2 blades. If only aerodynamic parked loads are considered, the turbine with a floating platform exhibits lower parked loads compared to turbine with a locked platform (fixed base) due to the effect of the tilted condition of the floating platform. Moreover, comparison between floating with wind and wave, and floating with wind only cases show that although both exhibits park loads of similar magnitude, the former exhibits more high frequency variation due to coupled effects of wind, wave, and floating platform dynamics. Additionally, we present a semi-numerical tool for estimating parked loads of VAWTs that we improved and validated to predict the floating parked loads. The analytical model accurately predicts the parked load behavior of VAWTs for the range of effects noted above. The datasets from this experimental work can serve as benchmarks for validating other computational parked load estimating tools, while the semi-numerical tool provides way to gain insight into the unmeasurable quantities.

1 Introduction

Vertical axis wind turbines (VAWTs) are gaining attention as a candidate for offshore deployments, especially in deep waters where floating platforms are required. Floating VAWTs have the potential to significantly reduce the cost of energy compared to floating horizontal axis wind turbines (HAWTs) [Shelley et al. (2018)]. Additionally, VAWTs have a lower center of gravity which helps to reduce the overturning moment.

One critical aspect of VAWT operation and deployment is understanding the design loads for parked or standstill conditions. Parked loads refer to the forces exerted on a wind turbine when it is in a stationary or non-operational state, such as during

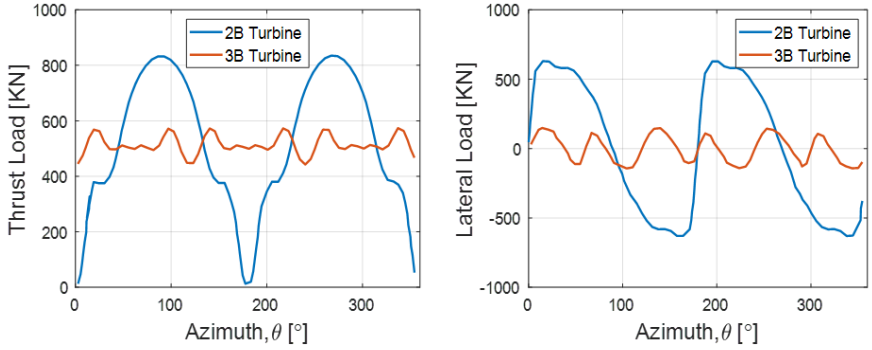

Figure 1. Parked loads on 5MW Darrieus VAWT at 30.64 ms^{-1} wind speed [Sakib and Griffith (2022)]

maintenance, low wind conditions, or shutdown scenarios. These loads are influenced by various factors including wind speed, solidity, number of blades, wind-wave-platform conditions, and the azimuthal position in a revolution.

Accurate assessment of parked loads is essential for several reasons. When not employing a blade pitching mechanism, VAWTs are subjected to high parked loads for extended periods. Sakib and Griffith (2022) showed that the magnitude of parked loads is similar in magnitude to the operating loads. A sample parked load with respect to azimuth at 30.94 ms^{-1} wind speed for a 5 MW UTD-designed VAWT is shown in Figure 1. Assessing parked loads would ensure the structural integrity and longevity of the wind turbine and floating system, preventing potential damage that could occur when the turbine is not generating power. Finally, understanding these loads contributes to optimizing the overall design and performance of VAWTs, making them more reliable and efficient.

To date, very few parked load studies of VAWTs are found in the literature. Sakib and Griffith (2022) analyzed parked aerodynamic load for a 5 MW conceptual VAWT, considering rotor design variables such as tapered blade chord, number of blades, aspect ratio (the ratio of rotor height to diameter). Although Sakib and Griffith (2022) numerically studied the effects of the number of blades on parked loads, in this study we have studied the effects of the number of blades on azimuthal variation of parkloads both numerically and experimentally. The analytical tool used in Sakib et al's study is validated here and improved by adding the capacity for estimating parked loads for offshore floating turbines. Ottermo et al. (2012) developed an analytical model to estimate extreme loads under parked conditions. Paulsen et al. (2013) conducted a CFD study to predict both the operating and parked load for the Deep Wind concept. Kuang et al. (2019) performed a numerical CFD investigation on the flow characteristics and dynamic responses of a parked straight-bladed vertical axis wind turbine (H-VAWT) and concluded that pressure distribution on the upwind blade surface are similar at different azimuthal locations. As wind speed increases, turbulent flow characteristics and wake effects become more pronounced, while dynamic responses due to parked conditions can be neglected. The only experimental parked load analysis of 12 kW VAWT was done by Goude and Rossander (2017), which used fixed base (locked platform) for an H-VAWT.

This study focuses on the experimental investigation of parked loads on vertical axis wind turbines with experiments performed in a wind-wave basin. The research aims to provide a comprehensive understanding of the factors affecting parked

loads and their impact on turbine performance. The findings from this study offer valuable insights for the design, operation, and maintenance of VAWTs, ultimately contributing to the advancement of sustainable wind energy technologies.

This paper also focuses on enhancing the capacity of UTD's (UT-Dallas) existing semi-numerical VAWT parked load estimating tool originally developed by Sakib and Griffith (2022). This tool make use of a mid-fidelity, open-source, free vortex method code CACTUS (Code for Axial and Cross-flow Turbine Simulation) [Murray and Barone (2011)] and analytical methods. CACTUS was developed by Sandia National Laboratories in FORTRAN 95 language using VDART3 [Strickland et al. (1980)] code as a basis. CACTUS code is capable of performing an analysis of any arbitrary turbine configuration by segmenting the turbine blades and struts into a set of blade elements. More detailed explanation of CACTUS can be found in Lu (2020).

In summary, the aim of this work is to experimentally study and validate the modeling of parked loads for Darrieus VAWTs with different platform conditions and to enhance the capacity of UTD's existing VAWT parked load estimating tool. The main contributions of this work can be summarized as below:

- An experimental study is performed that examines troposkein wind turbines with two blades (2B) and three blades (3B).
- The parked dataset presented here is unique because the data includes both fixed base (locked platform, zero tilting), and for floating platform conditions (floating with and without waves).
- Experimental data is gathered to validate a semi-numerical parked load estimating tool, originally developed by Sakib and Griffith (2022). The tool has also been improved to assess the parked load for offshore floating turbines with tilting. Ultimately this tool can be used to gain insights into the unmeasurable quantities.

Section 2 covers the methods for experiments, the test campaign, and the development of the parked loads model. Section 3 presents results and discussions for the experimental measurements and model validation efforts, with a focus on the effects of wind speed, turbine solidity (varying number of blades), different platform conditions, and effect of rotor azimuth. Section 4 presents the concluding remarks.

2 Methods

The VAWT rotors were tested at UMaine's Alfond Wind-Wave Ocean Engineering Laboratory (W2) [Cole et al. (2017)]. This unique facility is equipped with high-precision measurement instruments and allows for variable water depths, wind, and wave conditions. The basin measures 30 meters in length and 9 meters in width, with a maximum water depth of 5 meters. The wind machine, whose dimension is 7 m x 3.5 m, can generate up to 12 ms^{-1} wind speed using a narrower condenser passage; however, during these VAWT tests, maximum wind speeds were limited to 4.96 ms^{-1} with a turbulence intensity of 3.9%, since the condenser was removed. A detailed description of the testing facility can be found in Parker (2022) .

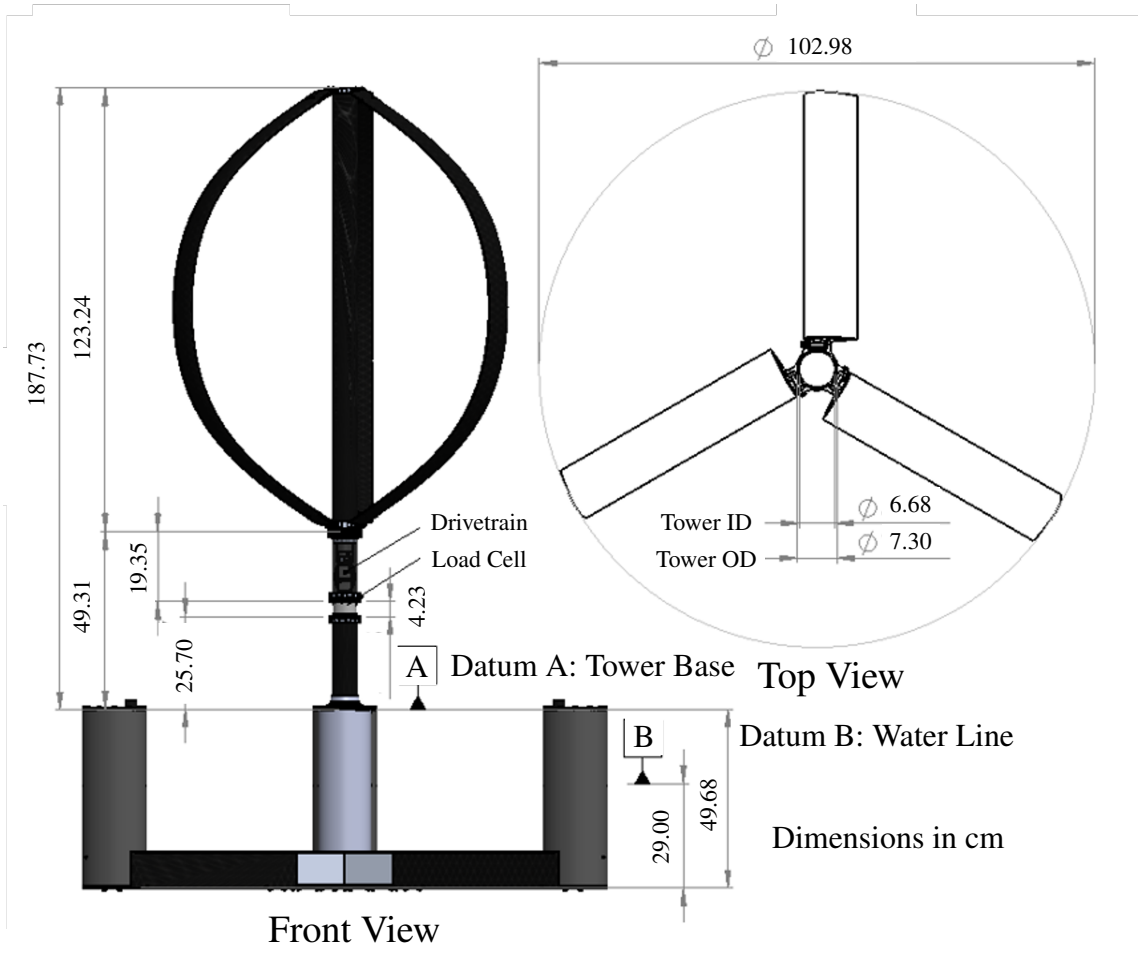

Figure 2. Visual of the 3B test turbine configuration CAD model with dimensions

2.1 Test turbines

Two scaled turbine configurations were tested at the test facility. These turbines are designed based on the constraints and requirements of the wind wave basin test facility, as well as constraints imposed by the floating system and safety requirements. For example, turbine dimension must not exceed the dimension of wind generating machine (W 7.0 × H 3.5 m). Both the turbines were alternately mounted on a floating platform which was originally used for FOCAL horizontal axis wind turbine. Details of the floating platform can be found in Robertson (2023). The turbines are also designed in a way that they maintain the load constraints implemented by the FOCAL platform. The rotor mass and overturning moment must not exceed 12.6 kg and 15.54 Nm, respectively. The overturning moment is defined as the multiplication of thrust force with the distance from mean water level to the center of pressure of the rotor. Moreover, the design met international structural safety requirements

Table 1. Geometric configurations of two tested troposkein turbines

Parameter	2B Turbine	3B Turbine
No of blades [-]	2	3
Airfoil chord, [m]	0.1	0.1
Rotor radius, [m]	0.515	0.515
Height to radius, [-]	2.5	2.5
Solidity, NC/D [-]	0.194	0.291

from the international design standards of composite wind turbine blades stated in Germanischer (2010). For detailed design of these model scale VAWTs, readers are referred to Hossain et al. (2024).

Both tested VAWTs have identical geometric properties, except for the number of blades. One turbine has two blades, whereas the other has three blades. The shape of the turbine is troposkein with equatorial radius of 0.515 m, and height of 1.287 m. It is configured with NACA0018 airfoil of constant chord length of the airfoil is 0.1 m. The solidity of 2B turbine (two-bladed, 2B) and 3B turbine (three-bladed, 3B) are 0.194 and 0.291, respectively. In this work, the solidity of the turbine is defined as NC/D, where N is the number of blades, C is the chord length, and D is the maximum diameter of the turbine. The solidity was varied only by changing the number of blades in order to limit the manufacturing complexity and cost. It was easy to convert the 2B turbine into the 3B turbine using one set of blades. The summarized geometric parameters are listed in the Table 1.

A schematic of the test turbine configuration CAD model with dimensions is shown in Figure 2. The image shows both front and top view of a 3B turbine. The dimensions of the 2B turbine are the same except for the number of blades.

2.2 Measurement system and data post processing

An ATI Mini58 (SI-700-30 calibration) six degree of freedom (6DOF) load sensor was used to measure the loads and moments. The load cell can measure maximum thrust of 700 N, maximum overturning moment of 30 Nm, and maximum torque of 30 Nm which meet the expected loads and moment requirements. The load sensor was placed in the tower base, please see Figure 2 for relative position. Table 2 lists the measurement systems for this experimental testing campaign. The rotor speed was measured using a motor encoder. And the platform dynamic motions (pitch/roll) were recorded using a Qualisys 6DOF a motion measuring system.

The testing facility and turbine design did not include the measurement of blade azimuthal tracking. Therefore, before every test, blade number 1 was placed at zero-degree azimuth position located at the most upwind position. Then the azimuth variation was tracked running the turbine at a constant and low speed of 1 RPM.

Table 2. Measurement systems for the experimental testing campaign

Item	Measuring tool
Loads and moments	6 DOF load sensor
Rotor speed	Motor encoder
Platform pitch/roll	Qualisys 6DOF motion

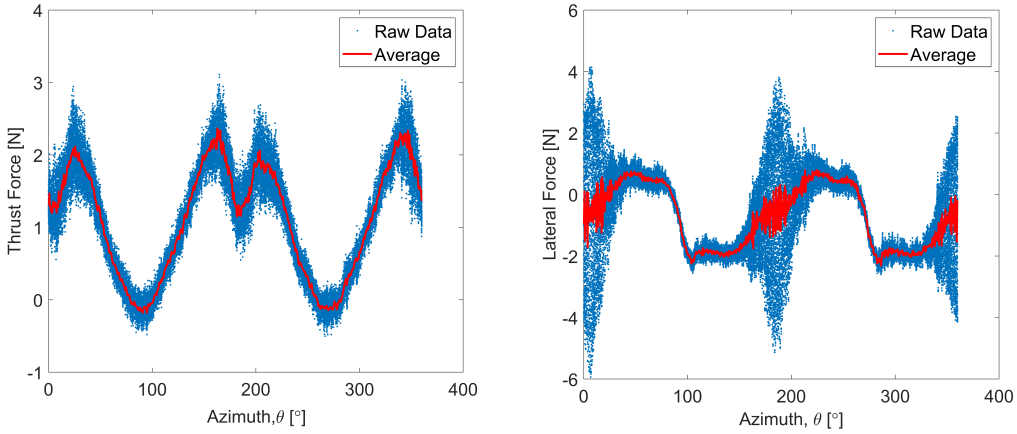

Figure 3. Comparison of raw and post processed average thrust and lateral loads at 2 ms^{-1} for the fixed base 2B turbine.

Before starting every measurement, the system data was recorded at non-running/pre-load condition to know if there were any residual values. After that, the fan was switched on to generate the specified wind speed. Then, after steady-state wind speeds were present, the turbine was rotated at 1 RPM and the raw load data was recorded.

For each test, the data was recorded for at least 5 revolutions. After recording the load data, the raw data was post-processed to exclude the startup (standstill to 1 RPM) and end (1 RPM to standstill) values. After that, the pre-load data was subtracted from the load condition raw data to get the actual true measured data. For averaging the raw data, a binning technique was applied. The azimuthal locations (from 0° to 360°) were divided into 720 bins. Data for all the revolutions are stored in the bins, which indicates that data were comparted in a way that every data for 0.5° azimuthal locations data goes into a single bin. Then the binned data are averaged to get the final post processed data of 720 azimuthal locations.

Figure 3 shows a sample comparison between raw and the post processed averaged parked thrust and lateral loads at 4.96 ms^{-1} wind speed for fixed base 2B turbine. The blue points indicate the raw data, and the red continuous line indicates post processed averaged data. This paper made use of the post processed averaged load data for all analysis thereafter.

2.3 Test matrix in the test campaign

The test matrix consists of 4 important variables which have the largest impacts on the parked loads of floating VAWTs. The first variable we considered is azimuthal position. The parked loads of VAWTs highly depend on the azimuthal positions. Figure 5 shows the azimuthal angle convention used in this study. 0° azimuthal positions represents that the first blade is in the windward direction. The turbine rotates anticlockwise.

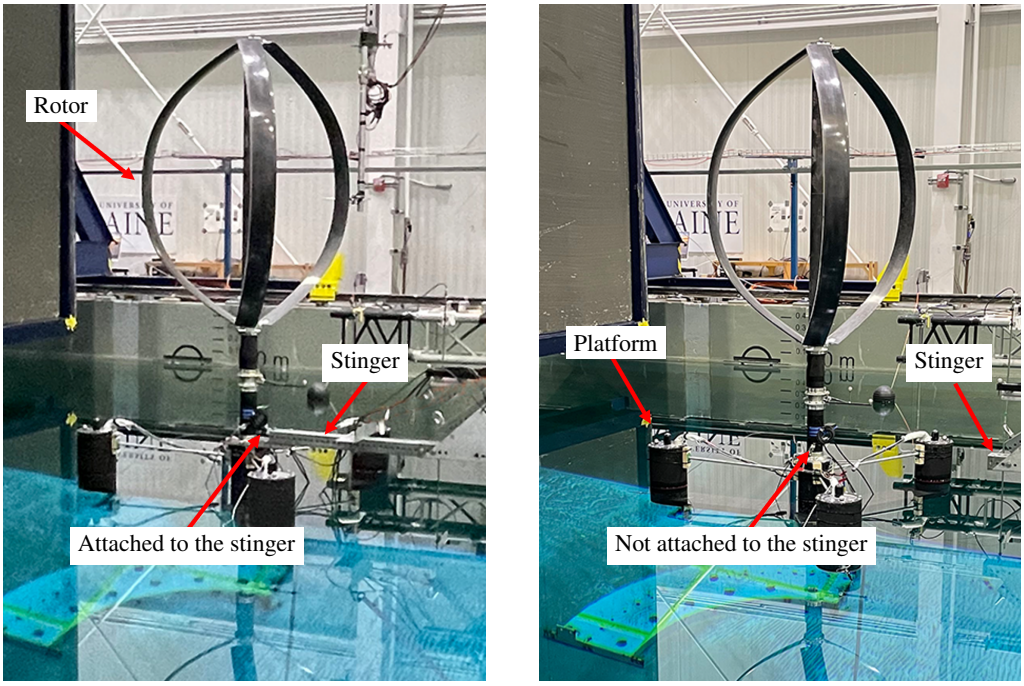

(a) Fixed base (b) Floating base

Figure 4. Tower base options used in the experiments.

The second variable we considered is wind speed. The test facility is capable of producing a maximum of 4.96 ms^{-1} wind speed. Therefore, the turbines were tested at wind speeds varied between 2 ms^{-1} to 4.96 ms^{-1} keeping the turbine rotational speed constant at 1 RPM. Geometric comparison of the test turbine (having radius of 0.51 m) to the UTD 5 MW VAWT [Sakib and Griffith (2022)] (having radius of 54.011 m) reveals that the test turbine is a 1:104.87 scaled version of the full-scale UTD 5 MW turbine. However, the test turbine is not a scaled design of the UTD 5 MW VAWT; this comparison is made solely to estimate the full-scale wind speeds. Applying Froude scaling with a velocity scale factor of $\lambda^{0.5}$ results in a wind speed range of 20.48 ms^{-1} to 50.79 ms^{-1} for full-scale 5 MW UTD VAWT. This wind speed range is reasonable because the site specific 50 years return period having a 10 minutes average wind speed of 30.96 ms^{-1} [Sirnivas et al. (2014)] falls in between this range.

The third variable considered in this test campaign is the number of blades. The two-bladed turbine (2B) has solidity of 0.194, whereas the three-bladed turbine (3B) has solidity of 0.291. The geometric configurations and visual representation of

Table 3. Test matrix

Variables	Short Description
Azimuth	Azimthal position ranges from 0° to 360°. The position of first blade in the wind ward direction represents the 0° azimuthal position.
Wind Speed	Wind speeds are varied between 2 and 4.96 ms^{-1}.
Number of Blades	Two-bladed (2B) and three-bladed (3B) troposkein VAWTs are tested in this campaign. 2B turbine and 3B turbine have solidities of 0.194 and 0.291, respectively.
Twind-wave-platform conditions	Three wind-wave-platform conditions were considered in the test campaign. Those are locked with wind only, floating with wind only, and floating with wind and wave cases.

tested turbines are shown in Table 1 and Figure 2, respectively. The detailed design and manufacturing of the turbines can be found in Hossain et al. (2024).

The fourth variable we considered is the wind-wave-platform conditions. The turbines were tested for three wind-wave-platform conditions: a) locked (fixed tower base) with wind only, b) floating with wind only (no waves), and c) floating with wind and waves. The locked with wind only condition represents a case where the tower base is attached to a stinger to restrict tilting motion (i.e., fixed base), and the turbine is rotated only in presence of wind with no waves present. Please see Figure 4 for details of the tower base attached to the stinger. The floating with wind only condition makes use of a semi-submersible floating platform. The column of floating platform is connected to horizontal mooring lines (not shown in the Figure 4) to keep the floating platform in place. However, the mooring lines were not connected to the basin bed. Instead, they were connected to the side wall to reduce the movement for this specific wind wave basin. In this condition, the turbines are only exposed to the wind. The floating wind and wave condition also uses the semi-submersible floating platform; however, the turbines are exposed to both wind and waves. In this test campaign, a regular wave with a height of 0.155 m and a period of 1.61 s is used, which corresponds to a full-scale IEA 15 MW horizontal axis wind turbine with a height of 10.85 m and a period of 13.5 s [Fowler (2023)]. Readers are referred to Figure 4 for the visuals of locked and floating platforms and referred to Table 3 for the test matrix used in this campaign.

2.4 UTD's semi-numerical parked load tool

A semi-numerical parked load tool is developed to estimate the parked loads of the tested turbines. As methods like CFD will be very computationally intensive to predict parked loads, a semi-numerical method has been developed with goals of accuracy and low computational effort. This tool makes use of static airfoil polar supplied with the CACTUS tool. Airfoil polars are applicable to VAWT operations, and they range from -180° to 180° of angle of attack. This tool makes use of static

airfoil polar supplied with the CACTUS tool. Use of static airfoil polars makes sense for the fixed-base system. For the two floating cases, we've performed analysis of reduced frequency to see if the inflow is steady or unsteady. Reduced frequency is a non-dimensional number, and it is defined in Matha et al. (2016) as follows:

$$K_i = \frac{\omega_{\text{ptfm}} C_i}{2\sqrt{U_\infty^2 + r_i^2 \Omega^2}} \tag{1}$$

where, ω_{ptfm} is the platform pitching frequency, C_i is airfoil section chord, U_∞ is freestream velocity, r_i is section radius, Ω is rotational velocity of rotor. According to Theodorsen theory, a flow can be categorized as unsteady if reduced frequency K in Equation 1 exceeds 0.05. The reduced frequency (K) does not go above a value of 0.05 for both floating wind only and floating wind wave conditions for any of the wind speeds for either 2B or 3B wind turbines. The highest reduced frequency (K) of 0.0158 occurs in the 3B floating wind wave pitch case. As wind speed increases, the reduced frequency decreases. Specifically, for the 3B floating wind wave pitch case, the reduced frequencies (K) at wind speeds of 2, 3, 4, and 4.96 m/s are 0.0158, 0.0105, 0.0079, and 0.0063, respectively. This indicates that higher wind speeds result in a steadier inflow. Therefore, the inflow can be considered quasi-steady, and the use of static polar for floating cases also makes sense. Since the induction due to blade wake is small compared to freestream velocity, and to make the model simpler, blade wake effects have been excluded from the model. Moreover, strut effects, and finite aspect ratio corrections have also not been considered.

The local relative velocity and angle of attack for all the azimuthal locations were calculated using CACTUS. In the relative velocity calculation, we only considered local free-stream velocity ignoring the rotational and induced velocity components because the rotor is standstill for the parked condition. However, induction due to tower wake was considered in the model as it was easy to implement in the model.

$$V_N = N_x U_x + N_Y U_Y + N_Z U_Z \tag{2}$$

$$V_T = T_x U_x + T_Y U_Y + T_Z U_Z \tag{3}$$

where the V_N and V_T are the normal and tangential velocity. U is the freestream velocity. N, and T are normal vector component and tangential vector component, respectively. The value of normal vector component (N) and the tangential vector component (T) are calculated using the 3D vortex-based code CACTUS. The directions of forces and velocities are shown in Figure 5. Where the 0° azimuth is in wind ward direction. The thrust load (F_{Th}) is in wind ward direction and the lateral load (F_{Lat}) is normal to the thrust load. The normal force (F_N) is toward the center and tangential force (F_T) is in the tangential direction of airfoil. Local relative velocity is calculated as,

$$V_R = \sqrt{[V_N]^2 + [V_T]^2} \tag{4}$$

After that, the angle of attack (α) is calculated from the normal and tangential components of the velocity.

$$\alpha = [Tan]^{-1}(V_N / V_T) \tag{5}$$

Then the lift (C_L) and drag (C_D) coefficients for respective angle of attack are calculated using the static airfoil polar supplied with CACTUS tool. After that, the local normal (C_N) and tangential (C_T) force coefficients are calculated using C_L and C_D

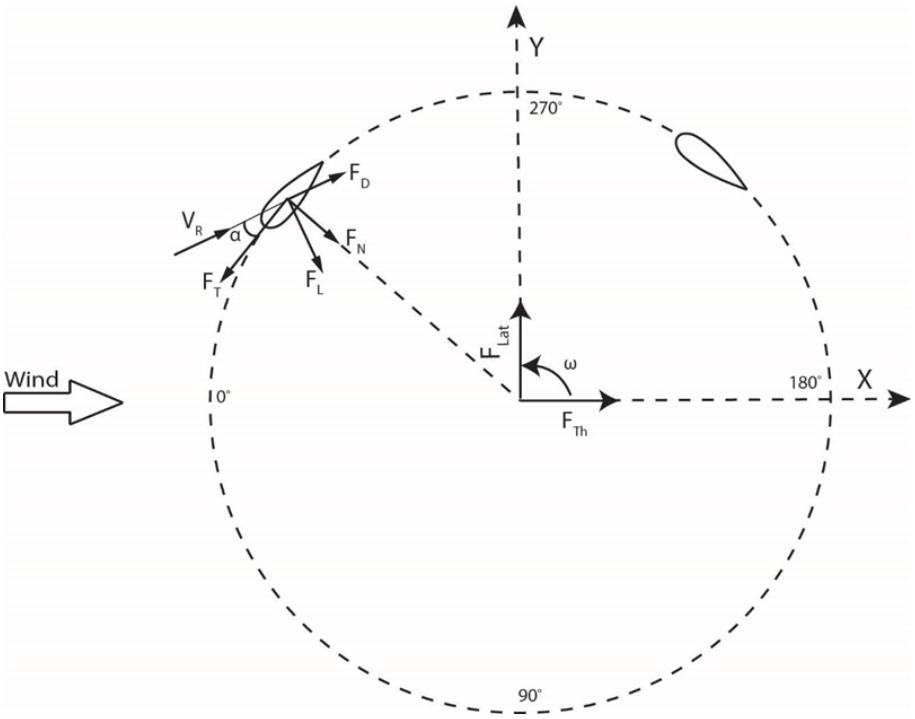

Figure 5. VAWT forces and velocities

as follows:

$$C_N = C_L\, Cos(\alpha) + C_D\, Sin(\alpha) \tag{6}$$

$$C_T = C_L\, Sin(\alpha) - C_D\, Cos(\alpha) \tag{7}$$

where C_L represents lift coefficient, and C_D represents drag coefficient. The normal and tangential force coefficients are local, in other words with respect to the specific element.

Therefore, normal and tangential force coefficients need to be re-referenced to full turbine scale to calculate the thrust and lateral forces. The conversion is done using the following equations.

$$C_{FtN} = C_N\, (A_E/A)\, (V_R/U)^2 \tag{8}$$

$$C_{FtT} = C_T\, (A_E/A)\, (V_R/U)^2 \tag{9}$$

where A_E is element area, A is rotor area, C_{FtN} and C_{FtT} are normal and tangential force coefficients w.r.t. rotor, respectively. After that thrust (C_{Th}) and lateral (C_{Lat}) force coefficients are calculated applying specific normal and tangential directions in the azimuthal locations.

$$C_{Th} = N_x\, C_{FtN} + T_x\, C_{FtT} \tag{10}$$

$$C_{Lat} = N_Y\, C_{FtN} + T_Y\, C_{FtT} \tag{11}$$

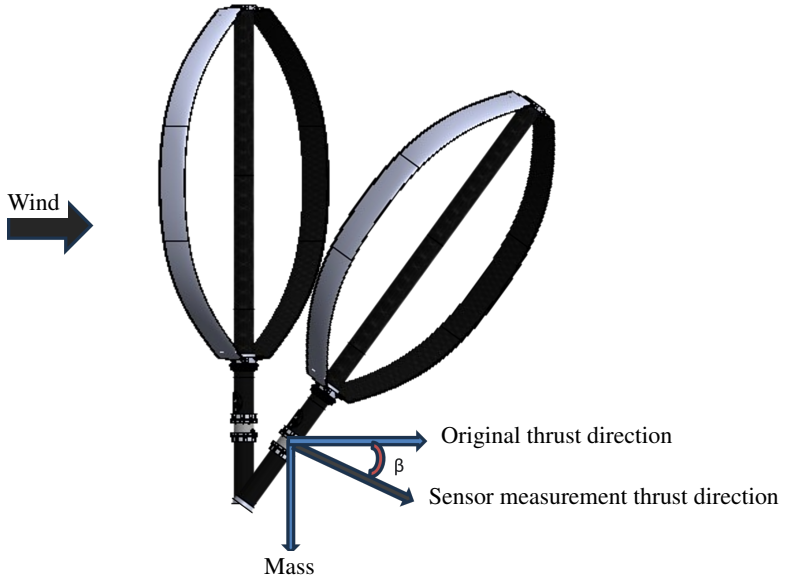

Figure 6. Schematic of gravitational effect on floating VAWT due to tilting.

Thrust and lateral loads for locked platform case,

$$F_{Th} = 1/2\,\rho A\,C_{Th}\,U^2 \tag{12}$$

$$F_{Lat} = 1/2\,\rho A\,C_{Lat}\,U^2 \tag{13}$$

A more detailed description of semi-numerical park load tool for fixed base VAWTs can be found in Sakib and Griffith (2022). The model also captures the tower drag. Tower drag is estimated using Equation 14.

$$F_{DTower} = 1/2\,\rho\,A_T\,C_D\,U^2 \tag{14}$$

where A_T represents the frontal tower area, and C_D is drag coefficient. For this analysis, a tapered cylindrical tower with an assumed C_D of 1 was used. The measured thrust load for the locked platform case includes tower drag, while the lateral load does not account for it, as static tower drag force acts in the thrust load direction.

$$F_{ThM} = F_{DTower} + F_{Th} \tag{15}$$

The parked load estimating tool presented in Sakib and Griffith (2022) could only calculate the parked load for fixed base turbine. However, estimating park loads for floating offshore VAWTs is also important. The procedure of estimating park loads for floating offshore VAWTs is outlined below.

The parked loads for floating offshore VAWTs are directly correlated with the turbine dynamic motions. For example, updated sensor measurement thrust, and lateral loads are directly correlated with turbine pitch and roll motions, respectively. The detailed correlation of loads and turbine dynamic motions is shown in section 3.1.4.

The load cell is fixed on the tower base, please see Figure 1 for the load cell position. For the floating platform condition, the turbine tilts due to the coupled effects of wind load and floating system. Therefore, the load cell, which is fixed in the tower, also tilts the same as the turbine. Therefore, the load cell's measured loads will not be in the original thrust or lateral load direction. The measured park loads are in the tilted sensor measurement load direction. Readers are referred to Figure 6 to see the updated sensor measurement load direction. The figure only shows the updated sensor measurement thrust direction. The original thrust direction is in the windward direction. However, due to wind and wave loads the load sensor also tilts. Therefore, the measured data corresponds to the tilted updated sensor measurement direction. However, being consistent with the locked and floating platform terminologies, we will still call the floating parked loads as thrust and lateral loads.

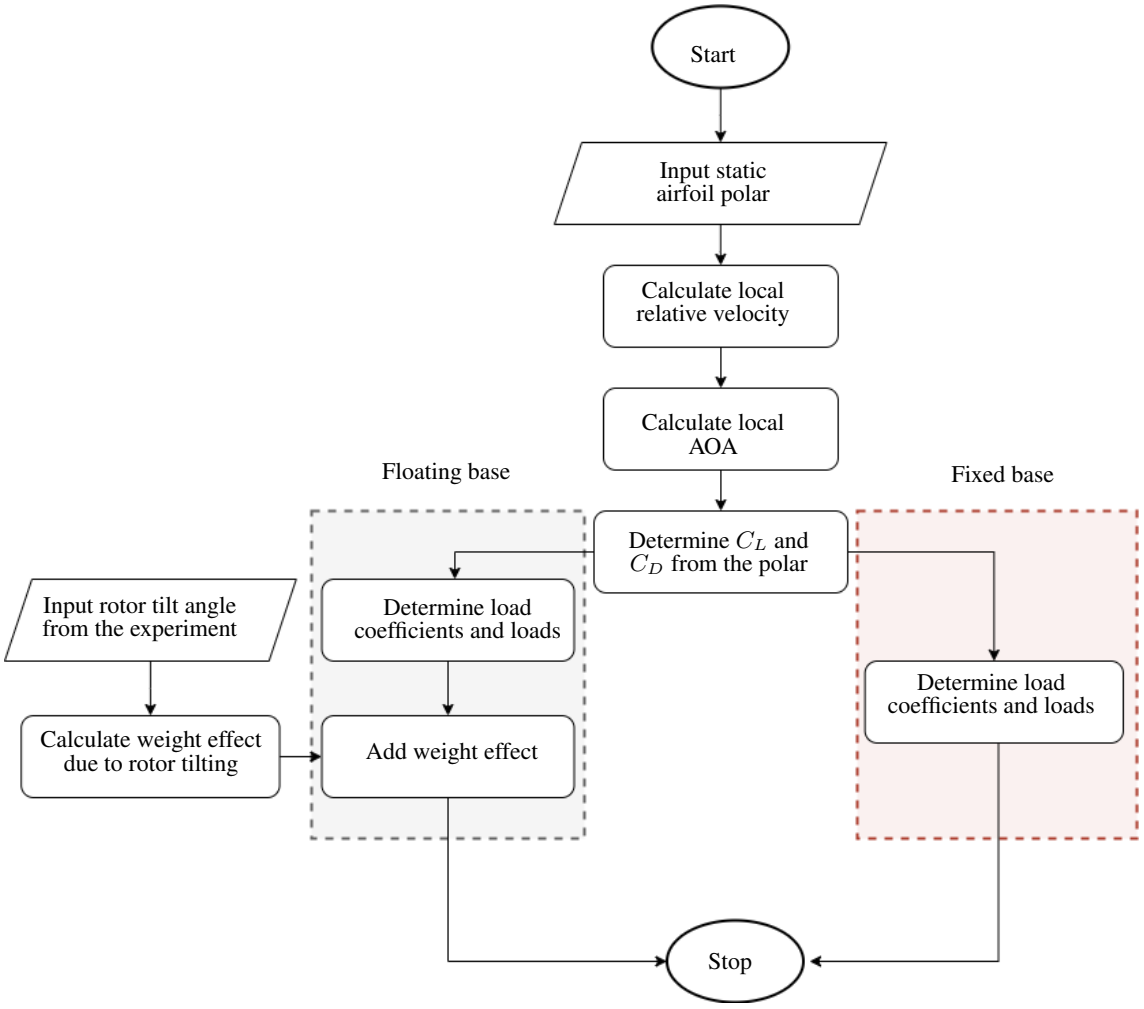

Figure 7. Flowchart of parked load estimating semi-numerical tool.

The semi-numerical parked load measuring tool takes this tilting effect into consideration by including the resulting inertial (weight) effect due to tilting. Due to tilting, the load sensor measures a component of weight, along with the loads (thrust/lateral)

in the original direction. Figure 6 shows the concept of the weight effect present in the floating thrust load. In the test campaign, both the loads and turbine dynamic motions were recorded. We used the measured pitch and roll data to calculate the weight effect. One can use the aero-hydro floating VAWT model developed in Gao et al. (2022) to predict the tilt angles as pre-test data for input to the parked loads model presented here. The input aerodynamic loads can be supplied using CACTUS, while the hydrodynamic coefficients can be obtained from a commercial software like WAMIT [Lee and Newman (2006)] or an open source code like Capytaine [Ancellin and Dias (2019)]. Then the aerodynamic model and hydrodynamic code can be combined with a mooring model to predict the tilt angles as done in Gao et al. (2022).

$$Weight\,(due\,to\,pitch) = M\,g\,sin(\beta) \tag{16}$$

$$Weight\,(due\,to\,roll) = M\,g\,sin(\gamma) \tag{17}$$

Thrust and lateral loads including both aerodynamic loads and weight effects for the floating platform case are given in the mode as follows:

$$F_{ThFl} = F_{ThM} + M\,g\,sin(\beta) \tag{18}$$

$$F_{LatFl} = F_{Lat} + M\,g\,sin(\gamma) \tag{19}$$

where β is measured pitch angle, γ is measured roll angle, M is turbine mass, and g is the gravitational acceleration constant.

A flowchart of the semi-numerical parked load calculation process stated above is also shown in Figure 7. This figure contains park load modeling of both the locked base and floating base platforms. The floating base case compensates for the tilting effect taking gravitational effects into consideration.

The UTD's parked load tool for the fixed tower base case has already been validated in Sakib and Griffith (2022). The extension of the tool for floating tower base case is discussed and validated in the results and discussion section of this paper.

3 Results and Discussion

3.1 Experimental data analysis

The main objective of this study is to quantify and model the effects of number of blades, wind speeds, wind-wave-platform conditions, and rotor azimuth on parked loads. This section will show and discuss the effects of these conditions successively.

3.1.1 Uncertainty in measurements

We perform an uncertainty analysis for the experimental measurements as follows [Coquilla et al. (2007)]:

$$U = \sqrt{(\beta^2 + (t\sigma)^2)} \tag{20}$$

where, U is resultant uncertainty, β is bias uncertainty, σ is standard deviation, and t is the coverage factor of T distribution. The value of t is 1.96 at 95% confidence level. Bias uncertainty of the load cell and anomometer are 0.1%, and 2%, respectively.

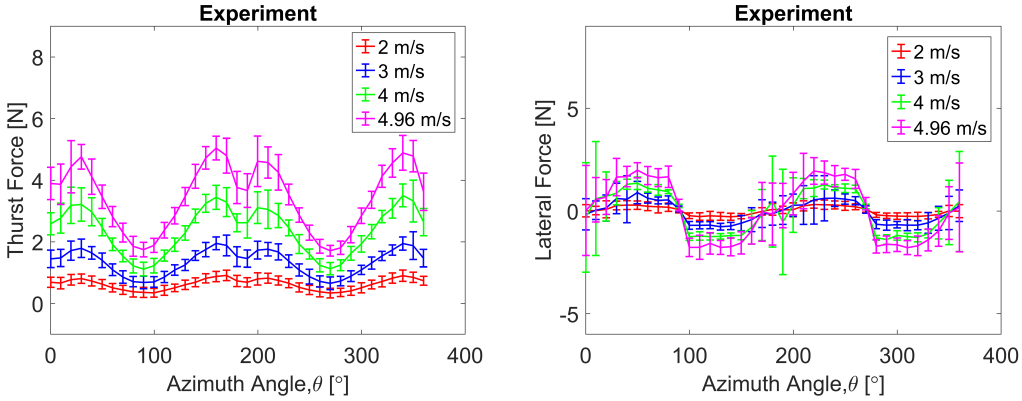

Figure 8. Parked loads with error bars of 2B turbine for locked wind only condition

Error bars for experimentally measured parked loads of the 2B turbine for the locked wind only case are shown in Figure 8. It is observed that the thrust load exhibits an uncertainty of approximately 10 to 15%, whereas the lateral load shows slightly higher uncertainty. Uncertainty levels are consistent across all measurements; therefore, in the interest of clarity in results presentation, the uncertainty bars have been excluded from the other plots.

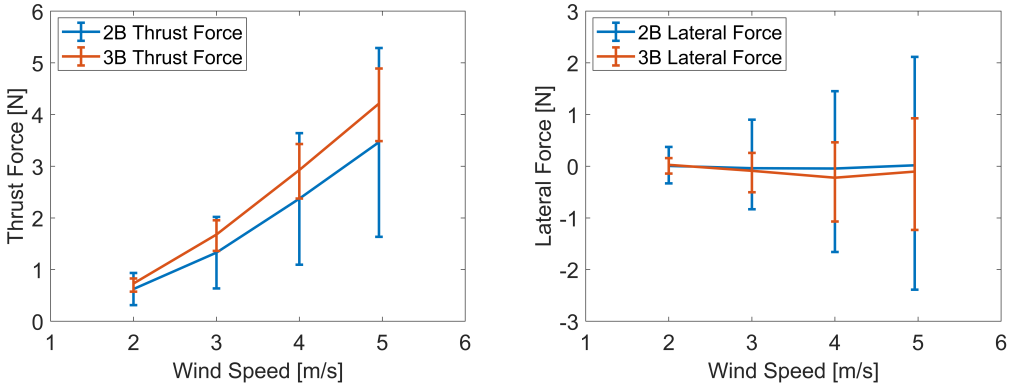

Figure 9. Effect of number of blades at locked tower base condition: a. thrust force b. lateral force. Note: horizontal bars shown are the variation in load due to azimuthal dependency, not uncertainty in the measurement.

3.1.2 Effect of number of blades variation

Both 2B and 3B floating VAWTs were tested in this test campaign. Variations in the number of blades, impacts the aerodynamic characteristics, structural dynamics, and overall efficiency of the turbine. For floating VAWTs, understanding the effect of the

number of blades on parked loads is essential to ensure stability and integrity under various operational and environmental conditions. This section explores the influence of the number of blades on parked loads, and their implications for floating VAWTs. Both 2B and 3B VAWTs were tested for fixed tower base and floating tower base conditions. However, the result is shown for the locked wind only case due to the fact that locked and floating platform conditions show a similar trend.

Figure 9 shows the parked loads as a function of wind speed for both the turbines. The horizontal bar in the figure shows variation due to azimuthal dependency, not uncertainty. It is observed that average thrust load increases with the increase in number of blades due to higher solidity and higher blockage to the incoming flow stated in Rezaeiha et al. (2018). Whereas, the number of blades effects are highly azimuth dependent. The variation (range) of thrust load due to azimuthal dependency in a particular wind speed decreases as the number of blades increases. The average lateral load is independent of the number of blades. It always stays at zero as wind has almost zero contribution in the lateral direction. However, the amplitude of lateral forces (load fluctuation for a particular wind speed due to azimuthal dependency) decreases as the number of blades increases which might be helpful for turbine structural integrity [Le Fouest and Mulleners (2022)].

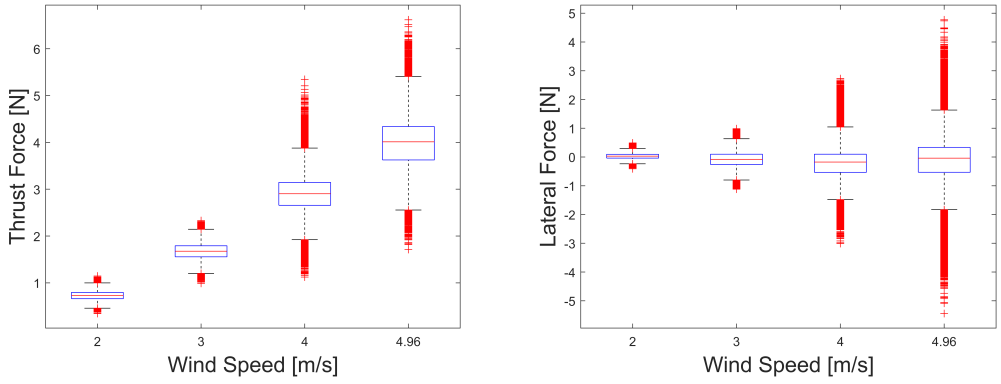

Figure 10. Effect of wind speeds on 3B turbine at locked tower base condition: a. thrust force b. lateral force

3.1.3 Effect of wind speeds

The parked loads of vertical axis wind turbines (VAWTs) are significantly influenced by wind speed. This section investigates the influence of wind speeds on the parked loads of VAWTs. To assess the impact of wind speeds on parked loads, a series of experiments were conducted using a scaled model of a floating VAWT. The turbines were exposed to wind speeds ranging from 2 to 4.96 ms^{-1} in a controlled wind tunnel environment. To keep the paper concise, this section only considers the parked loads on locked wind only condition. We skipped the effect of wind speed for 2B turbine due to the fact that the 2B turbine and 3B turbine show similar trend on parked loads. The impact of wind speeds on parked loads for 3B turbine through whisker box plot is shown in Figure 10. The figure shows the data for the locked wind only condition. The result indicates that the

Table 4. Wind-wave-platform conditions

Conditions	Short Description
Locked with wind only	Tower base/floating platform is connected to the stinger to restrict the tower base movement. The turbine is rotated azimuthally in the presence of only wind.
Floating with wind only	The floating platform is connected with horizontal mooring line. And the turbine is rotated azimuthally in the presence of only wind.
Floating with wind wave	The floating platform is connected with horizontal mooring line. And the turbine is rotated azimuthally in the presence of both wind and wave.

amplitude of lateral load and average thrust increase with the wind speed. The red dots indicate the outliers. The high number of outlier data is due to the variation of load with respect to the azimuth.

Current vertical axis wind turbine concepts usually exclude the complex pitching of blades that can be used to shed some load in higher wind speeds. Therefore, the loads increase with the wind speed is expected as no blade pitching was present in this study. The increase of parked loads with wind speeds can also be substantiated from the similar comments made in Carmo et al. (2024). This increase of parked loads with wind speed signifies that parked loads will be a crucial factor in high wind speed. Thus, wind turbine designers should focus on parked loads too, especially for high wind speeds.

3.1.4 Comparisons among different wind-wave-platform conditions

In this section, we compare the parked loads among the three conditions detailed in Table 4. In the locked (fixed tower base) wind only condition, the tower base is attached to a stinger to restrict all the tower base motion. In the floating wind only condition, the floating platform is connected to the mooring line. The mooring lines are horizontal line which are connected to the bottom of the floating platform columns and springs. The horizontal mooring was adopted to reduce the experimental uncertainty related to conventional catenary mooring [Ahsan et al. (2022)]. In the floating wind wave condition, the rotor was operated on a floating platform in the presence of both wind and waves.

In the test campaign, we measured the parked loads for 2, 3, 4, and 4.96 ms^{-1} for locked wind only and floating wind only conditions. Tests were conducted for both 2B and 3B turbines. However, parked loads at only 4 and 4.96 wind speeds were measured for the floating wind wave condition. Moreover, this case considered 3B turbine only, due to limitations of available testing time. The loads show similar characteristics for 2B and 3B turbines.

Offshore floating conditions often cause turbines to tilt, which has two competing effects: greater tilt reduces aerodynamic loads but increases weight effects. Experimental lateral load and thrust load comparison among different conditions are shown on Figures 11 and 12, respectively. The results shows that lateral load amplitude and average thrust load for floating conditions

is greater than the locked wind only condition. Although tilting in the floating case can reduce aerodynamic loads due to reduction in swept area and through damping effects [Ahsan et al. (2022)], the added weight component in the sensor's direction results in higher measured loads. When the turbine tilts, the six degree of freedom load and moment measuring sensor also tilts. This sensor tilting along with gravitational load measurement is shown in Figure 6. Thus, the measured data includes the lateral load component and weight load of the turbine due to rotor tilting. If we would consider the loads in the original thrust or lateral direction only, then floating with wind only and floating with wind wave cases would show the expected lower parked loads compared to the locked wind only case.

The lateral load amplitude and average thrust load for floating wind only and floating wind wave are almost the same (please refer to Figures 11 and 12). The only variation is that the floating wind wave data are noisier (or varied with high frequency) than the floating wind only condition due to the coupled dynamics of wind and wave. The high frequency variation is due to the high frequency (0.62 Hz) of the regular wave used in the experiment.

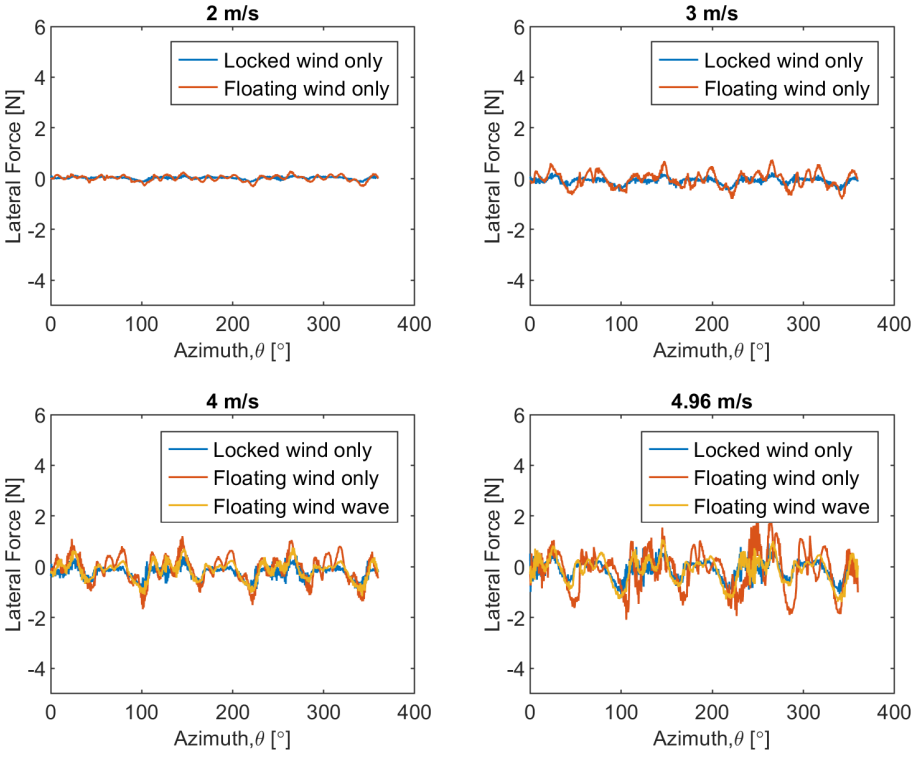

Figure 11. Experimental lateral load as a function of azimuth (3B Turbine) a. 2 ms^{-1} b. 3 ms^{-1} c. 4 ms^{-1} d. 4.96 ms^{-1}.

3.1.5 Correlation between parked loads and turbine dynamics

The correlation coefficient of two random variables is a measure of their linear dependence. If each variable has N scalar observations, then the Pearson correlation coefficient is defined as

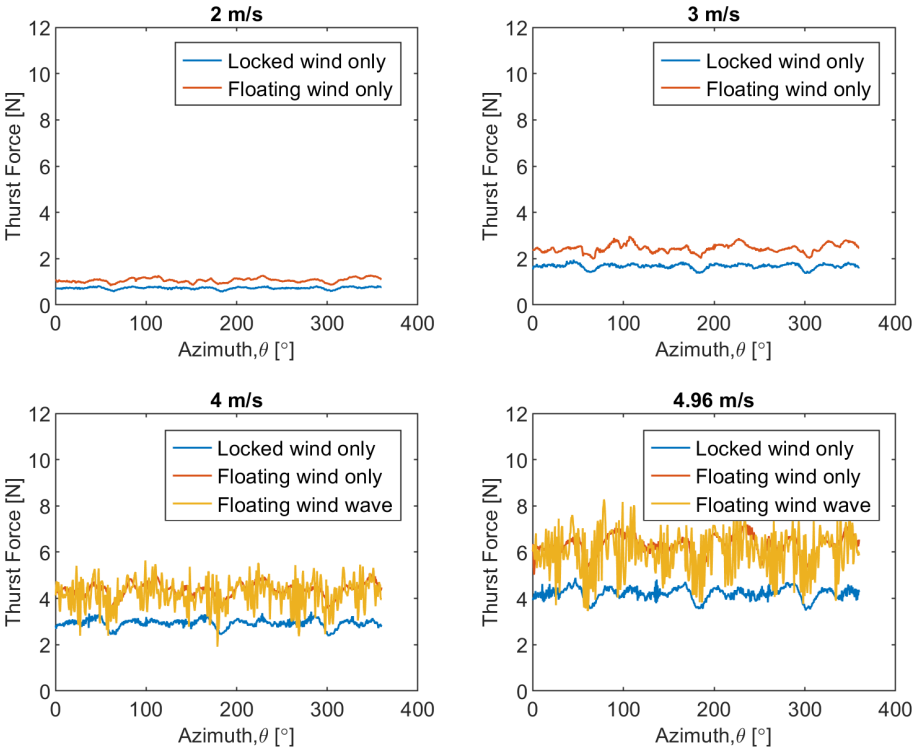

Figure 12. Experimental thrust load as a function of azimuth (3B Turbine) a. 2 ms^{-1} b. 3 ms^{-1} c. 4 ms^{-1} d. 4.96 ms^{-1}.

$$P(A,B) = \sum_{i=1}^{N}(A_i - \mu_A\sigma_A)(B_i - \mu_B\sigma_B) \tag{21}$$

where μ_A and σ_A are the mean and standard deviation of A, respectively, and μ_B and σ_B are the mean and standard deviation of B.

The loads and dynamic motions with respect to azimuthal position are shown in Figure 13 and Figure 14 for the lateral/roll and thrust/pitch loads/motions, respectively. The left Y axis represents the load, and right Y axis represents the tilt angle. The correlation coefficients between lateral load and roll motion for 2, 3, 4, and 4.96 ms^{-1} are -0.98, -1, -0.99, and -1, respectively. Whereas the correlation coefficients between thrust load and pitch motion for 2, 3, 4, and 4.96 ms^{-1} are 0.98, 0.99, 0.99, and 0.99, respectively. The coefficients shown here are for 2B tubine. It is seen that the dynamic motions and parked loads are highly correlated. Thrust load is highly correlated with pitch motion, whereas lateral load is highly correlated with roll motion. For the lateral loads/roll motion case, the negative correlation coefficient is simply due to the assumed lateral load and roll direction variation. This does not mean that as the roll angle increases, the turbine lateral load decreases.

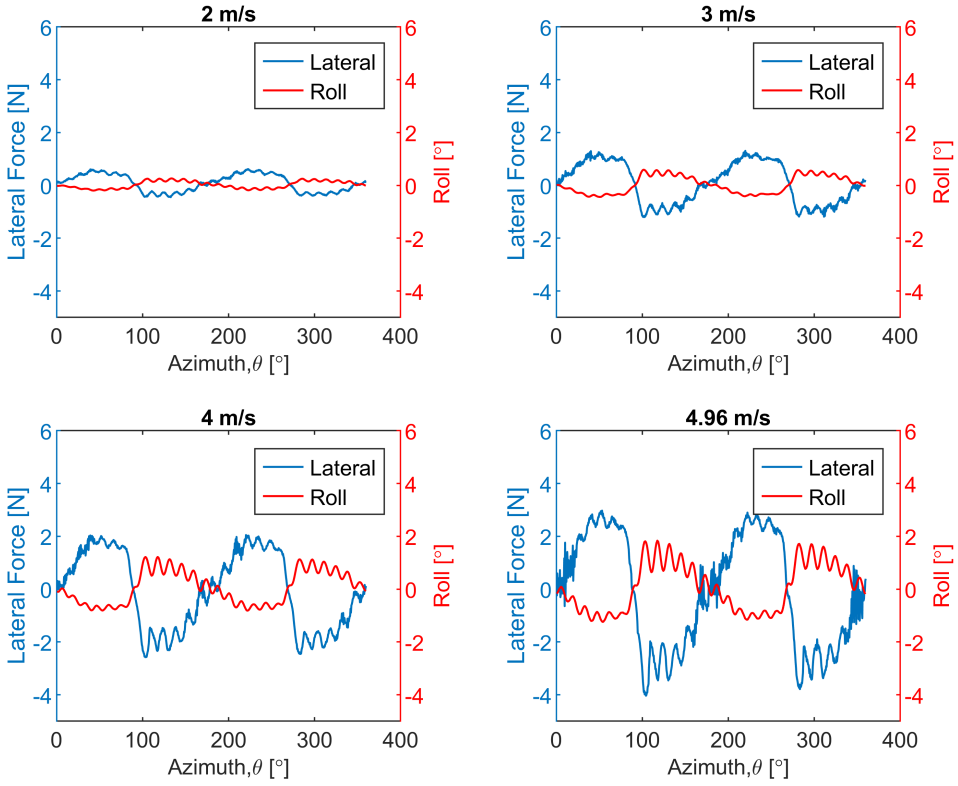

Figure 13. Experimental lateral load and dynamic roll motions in floating wind only condition for 2B turbine a. 2 ms^{-1} b. 3 ms^{-1} c. 4 ms^{-1} d. 4.96 ms^{-1}.

3.2 Semi-numerical parked loads model and validation

3.2.1 Locked wind only condition

This section compares parked loads from both the experiments and the semi-numerical model of two-bladed (2B) and three-bladed (3B) test turbines with locked tower base condition.

Figures 15 and 16 illustrate the variation of parked thrust and lateral loads with respect to azimuthal position for 2B turbine and 3B turbine, respectively. The experimental data represents the phase average of 5 revolutions, where the semi-numerical data is based on the last revolution values after the CACTUS simulation has converged. Figure 15a shows a comparison of non-dimensional forces, helping the evaluation of loads of different scale turbines, while Figure 15b shows a comparison of dimensional case, which applies exclusively to this test turbine. Analysis shows generally a very good agreement between experiments and our parked loads model in terms of both magnitudes and rotor azimuth dependence. Both thrust and lateral

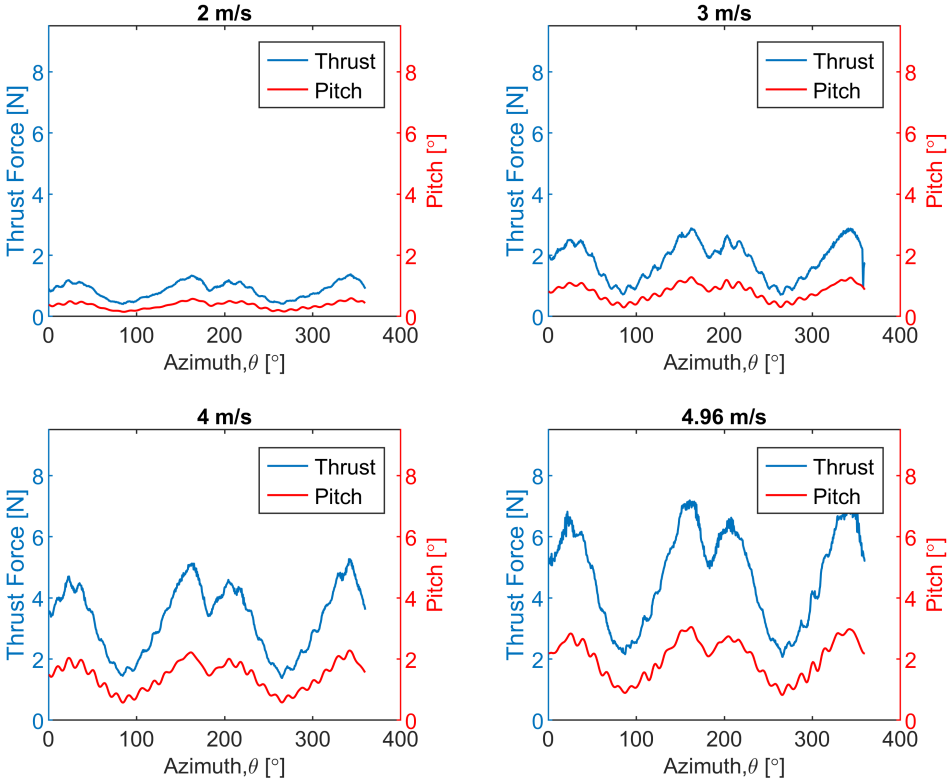

Figure 14. Experimental thrust and dynamic pitch motions in floating wind only condition for 2B turbine a. 2 ms^{-1} b. 3 ms^{-1} c. 4 ms^{-1} d. 4.96 ms^{-1}.

loads amplitudes increase with the wind speed increment. The sharp decrease of experimental thrust load at 180° azimuthal location is due to the tower shadow effect, which is captured well in our model.

Both experimental and semi-numerical results show a clear relationship between wind speed and thrust force: higher wind speeds generate larger thrust forces. The periodic nature of the thrust force with respect to azimuth angle is consistent for the experiments and model.

The lateral force increases in magnitude with the increase wind speeds, keeping the mean force at almost zero. Experimental results show measurement noise due to sensor inaccuracies and inherent variability in the system.The results from semi-numerical model appear smoother compared to measured data. Again, the overall trends of force variation are captured similarly by both the experiment and the semi-numerical model.

Thrust force shows (Figures 15 and 16) strong resemblance between experiment and model, although the experimental results include measurement noise. Both model and experiment capture the cyclic nature (2 cycles for the 2B turbine and 3 cycles for the 3B turbine in a revolution) of the forces with respect to the azimuth angle.

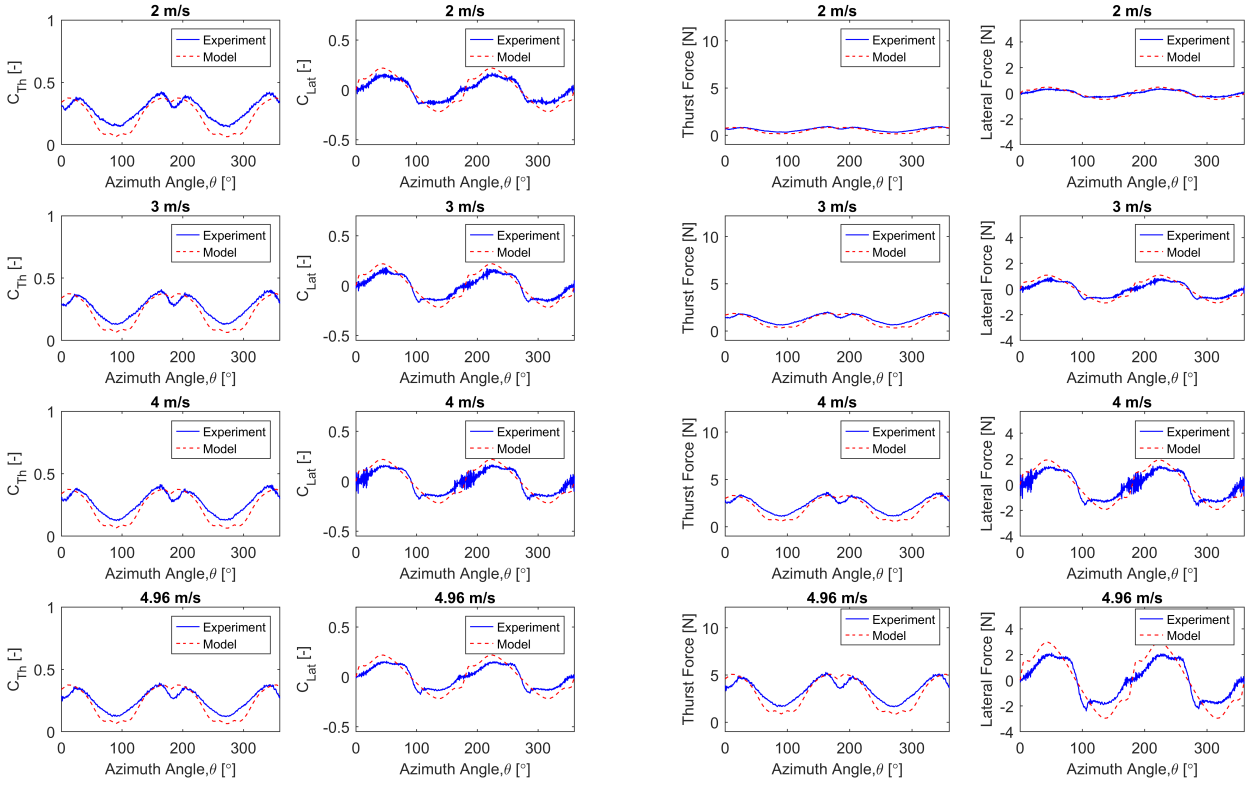

(a) Non-dimensional loads

(b) Dimensional loads

Figure 15. Comparison between experimental and semi-numerical parked loads of 2B turbine for locked with wind only condition

3.2.2 Floating wind only condition

Modeling the floating case with wind comes with a new challenge. The challenge is to model the weight effect due to rotor tilting in the floating tower base case, as well as capturing the impact of tilting on aerodynamic loads. A detailed description of modeling parked loads at floating tower base condition has been shown in section 2.

This section is intended to analyze the modeled parked load data for floating wind only case in the absence of waves. Due to the floating condition, the rotor tilts under wind loading. Which adds a component of rotor weight in the measured updated sensor thrust and lateral direction. The rotor weight was already measured in the wind wave basin. The 2B and 3B turbines weigh 5.97 kg and 6.55 kg, respectively. This mass includes only the components mounted above the load cell, including the blades and tower mass. The measured mass excludes the mass of the lower tower section, load cell, generator and hull.

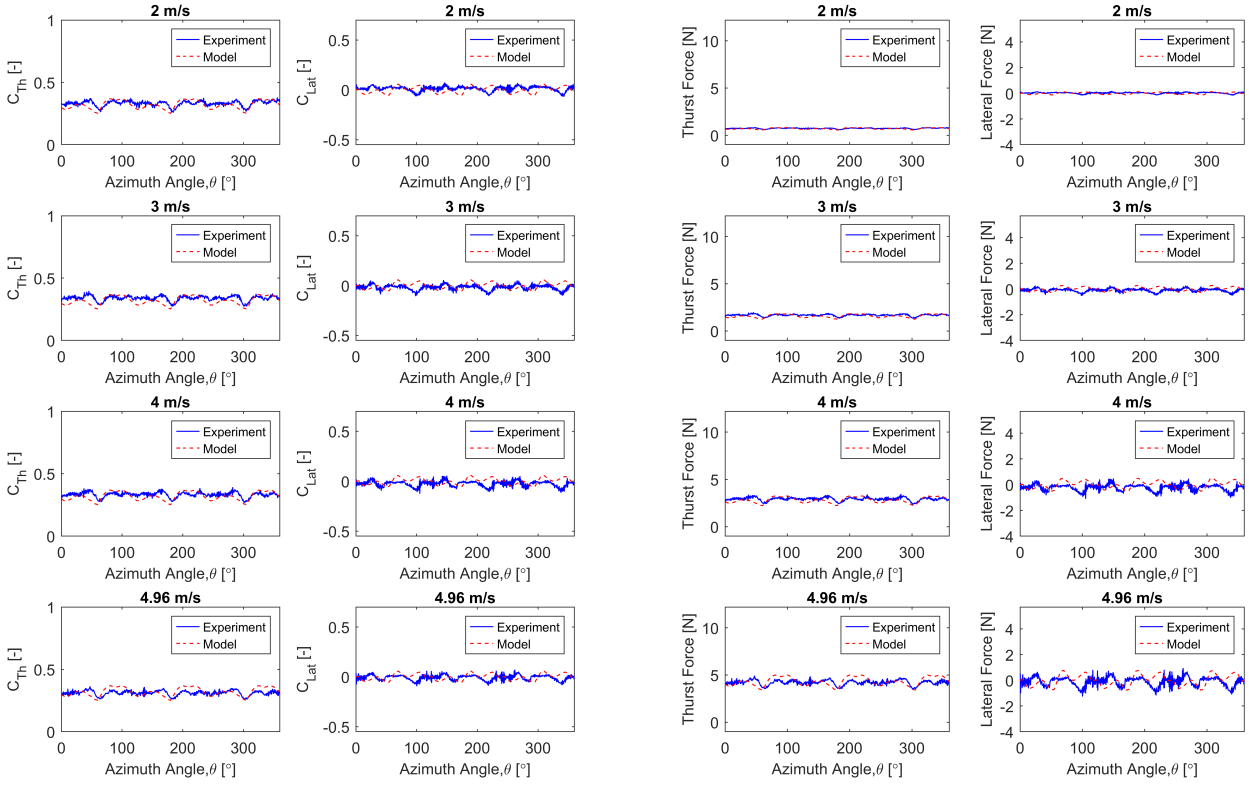

(a) Non-dimensional loads

(b) Dimensional loads

Figure 16. Comparison between experimental and semi-numerical parked loads of 3B turbine for locked with wind only condition

A representative weight effect in the thrust direction for the 2B turbine in the floating wind only condition is shown in Figure 17. This figure represents the pitch in red and turbine weight force in the measured thrust direction in blue. It is observed that, with the increase in wind speed, the weight effect also increases. It is a significant amount compared to the parked thrust load of similar wind speed. 2B turbine generates maximum thrust force of 5N at 4.96 ms^{-1} for locked wind only case. Whereas, the weight effect for the same turbine at the floating condition due to tilting at 4.96 ms^{-1} is 2.4 N, which is around 48% of the thrust load of the locked wind only case. Thus, including the rotor weight effect is very important while modeling the parked load for floating cases.

Figures 18 and 19 show the validation of UTD semi-numerical parked load with floating wind only condition for 2B and 3B turbines, respectively. The tool accurately predicts the trend for both thrust and lateral parked loads for the floating wind only case. However, the model slightly overpredicts the thrust load in some of the azimuthal locations, especially near 0°(360°) and 180° locations. Additionally, it underpredicts the lateral loads in certain azimuthal locations. The high frequency variation in

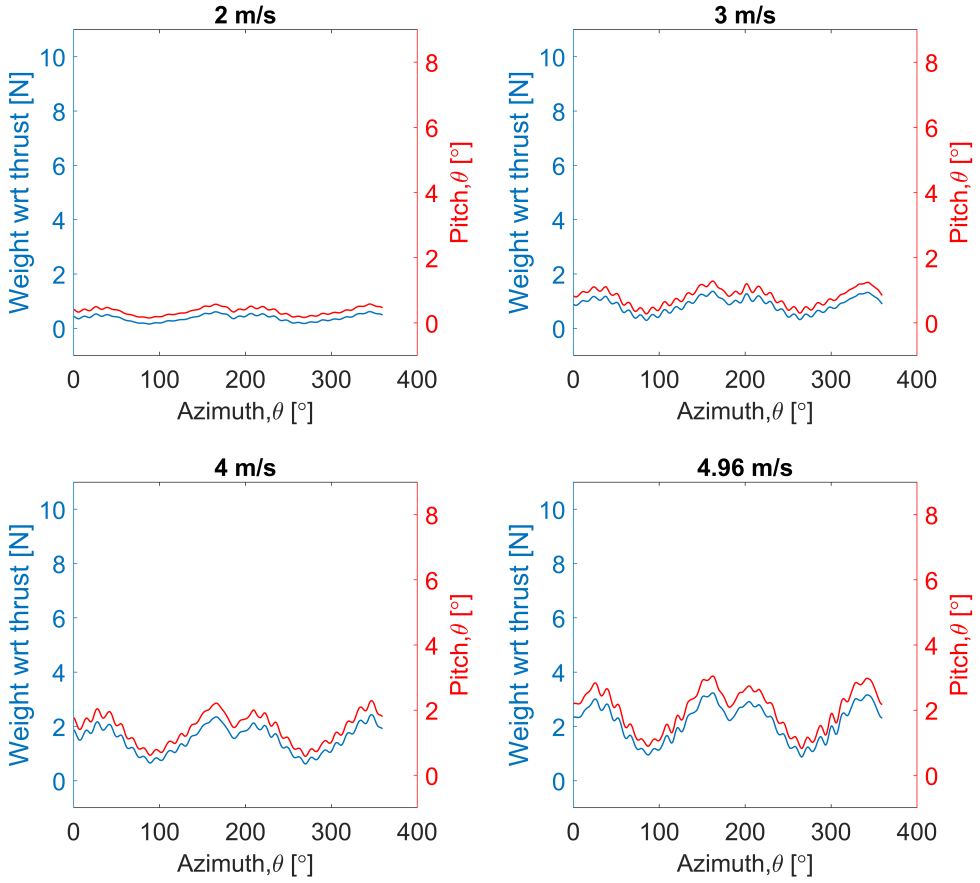

Figure 17. Weight effect in the thrust direction for 2B turbine in the floating with wind only tower base condition

loads, both in thrust and lateral parked loads, is due to turbine dynamics (roll/pitch) in the floating condition. The dimensional and non-dimensional plots show similar trends.

3.2.3 Floating tower base with wind and wave

We now examine the third configuration of the test, which is floating with both wind and waves. The turbine weight effect is also added with the fixed tower base parked load to calculate the parked load for wind and wave case. Regular wave with a height of 0.155 m and a period of 1.61 s is used to measure the parked load at floating tower base with wind and wave condition. And as the base is floating, it reflects a coupled effect due to wind, wave, and floating platform.

The validation in the case of floating with wind and wave case for the 3B turbine is shown in Figure 20. It is observed that the tool cannot properly capture the dynamic nature of pitch and roll and respective dynamic thrust and lateral loads due to coupled

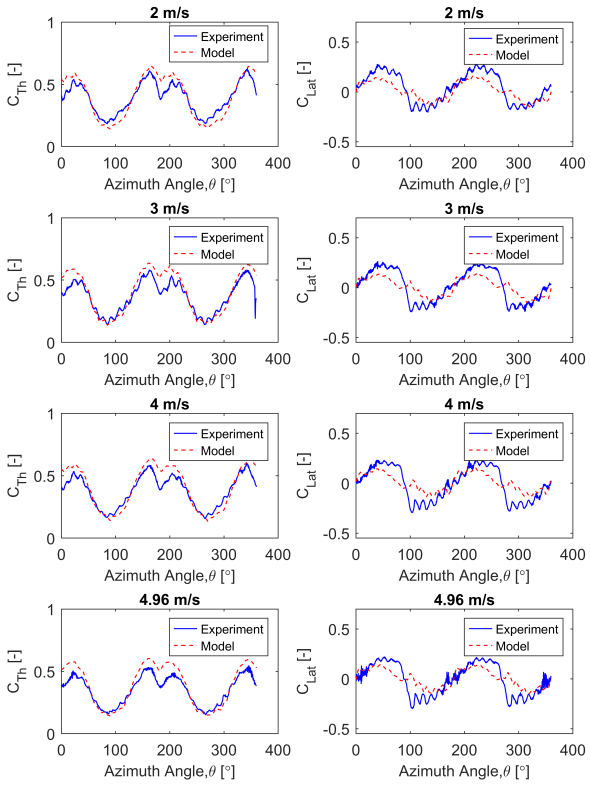

(a) Non-dimensional loads

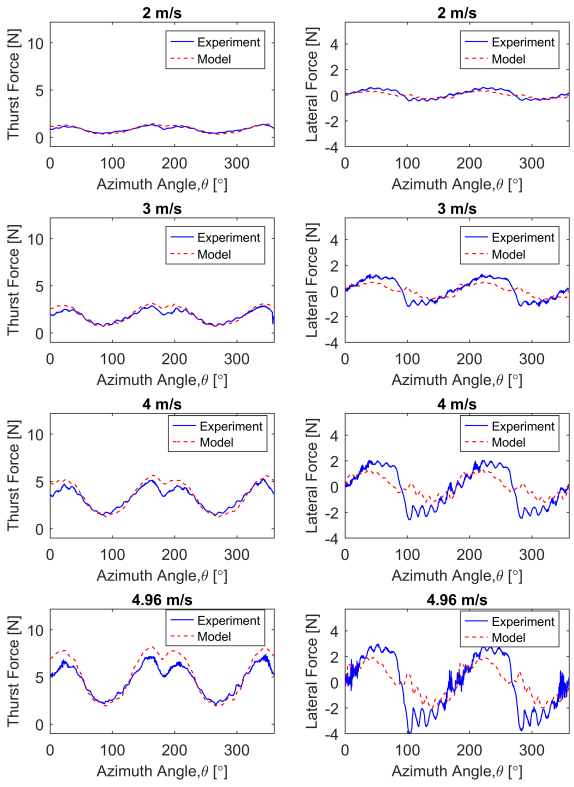

(b) Dimensional loads

Figure 18. Comparison between experimental and semi-numerical parked loads of 2B turbine for floating with wind only condition

wind, wave, and floating platform effects, although it does handle the static pitch and roll motions. A prediction of pitch and roll motions requires integrating aerodynamic, wave, hydrodynamic, platform and mooring dynamic models. A code, such as WAMIT [Lee and Newman (2006)], or an open source code Capytaine [Ancellin and Dias (2019)], can be used to model the hydrodynamics, then coupled with mooring and aerodynamics models to predict the platform motion using an aero-hydro model [Gao et al. (2022)]. Such a model can be used for pre-test motion prediction. Here, the authors have restricted their study to the current semi-numerical parked load model and comparison with the experimental data. Overall, the semi-numerical tool well predicts the magnitude of parked loads, azimuthal dependence on loads, and the effects of wind speed, and solidity for all the wind-wave-platform conditions. Additionally, this tool accurately captures the tower shadow at the 180° azimuthal location.

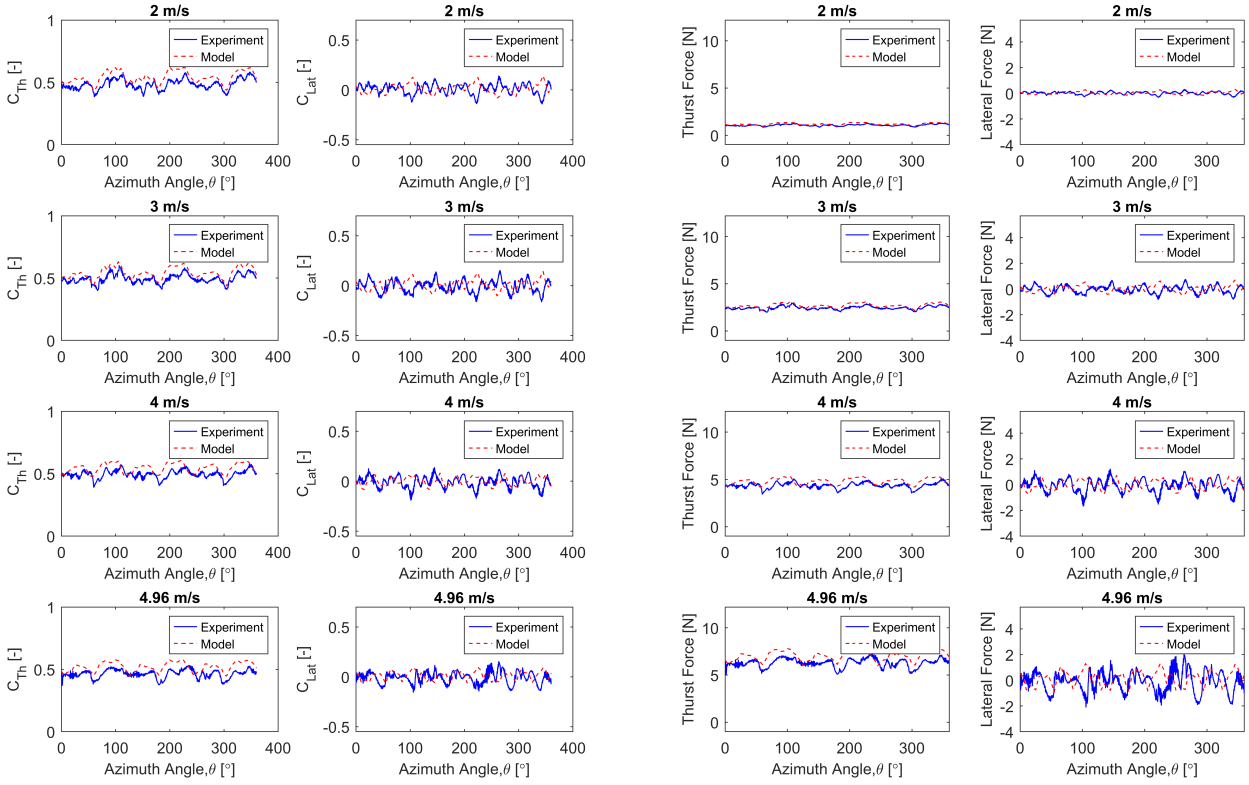

(a) Non-dimensional loads

(b) Dimensional loads

Figure 19. Comparison between experimental and semi-numerical parked loads of 3B turbine for floating with wind only condition

4 Conclusions

Floating offshore VAWTs are showing promise for deep water offshore locations as they offer several advantages including a lower center of gravity, thus improving stability and reducing the risk of overturning. However, some aspects in the design of floating VAWTs must be studied, including parked loads, which are comparable in magnitude to operating loads [Sakib and Griffith (2022)], are thus critical design loads, yet no studies have measured parked loads under floating conditions.

This study experimentally investigates parked loads on floating VAWTs in a wind-wave basin, aiming to provide insights on the factors influencing parked loads. Additionally, this study seeks to gather data to improve and validate a semi-numerical parked load estimation tool for floating VAWTs under both wind-only and wind-and-wave conditions that is based on a vortex aerodynamics model of the rotor and an analytical model of tower drag. Further, this model effectively captures the effects of tower shadow, azimuth dependence and weight effects.

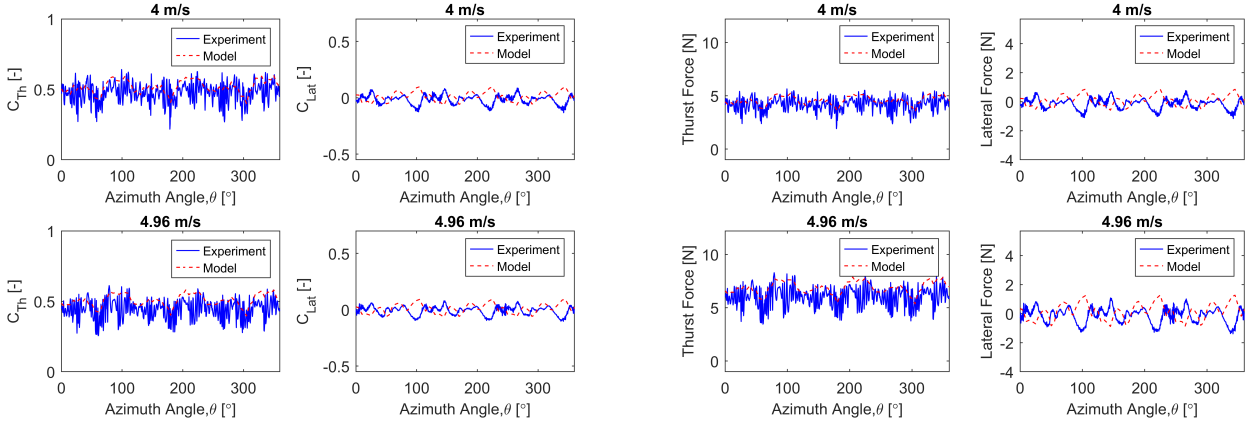

(a) Non-dimensional loads

(b) Dimensional loads

Figure 20. Comparison between experimental and semi-numerical parked loads of 3B turbine for floating with wind and wave condition

The study presents data on parked loads across varying wind speeds, solidity values, and wind-wave-platform conditions, examining the impact of gravitational loads from tilting and the correlation between tilt angles and parked loads. Validation of the semi-numerical estimation tool is also included.

The findings highlight the significance of wind speed, solidity, azimuth dependence, and wind-wave-platform conditions in determining parked loads for floating VAWTs. It was observed that VAWTs are subjected to substantial forces even in a stationary state, which necessitates robust structural designs to ensure their durability and safety.

The insights gained from this study underscore the importance of considering parked loads in the design phase of VAWTs. By incorporating validated parked loads models into the design process, engineers can develop more resilient turbines that can withstand the stresses encountered during non-operational periods. This is particularly crucial for enhancing the longevity and reliability of VAWTs, thereby making them a more viable option for renewable energy generation in diverse settings.The summary of the main findings of the paper can be stated as follows:

- Solidity (in terms of number of blades) influences the parked loads. The load variation (range) decreases as the number of blades increases.
- In floating conditions, average thrust load increases due to the gravitational load effect of turbine, while the amplitude of lateral load also increases.
- The floating wind-wave case exhibits more noisy loads due to dynamic nature compared to floating wind only case.
- The UTD's semi-numerical parked load tool quite accurately estimates the parked loads for both locked and floating platform conditions. It effectively captures the average load magnitude, load's azimuthal dependence, effects of wind speed, and number of blades. Tower shadow is also captured. However, this model is not formulated to predict the

dynamic nature of pitch and roll motions and respective dynamic thrust and lateral loads due to coupled wind, wave, and floating platform effects, although it effectively captures the average loads.

In conclusion, this study has advanced our understanding of the experimental parked loads on VAWTs and their impact on turbine performance. The results provide valuable guidelines for designing and implementing floating VAWTs that are both efficient and resilient. Future research should focus on further refining these findings through long-term field studies and exploring innovative materials and design strategies to mitigate parked loads. By addressing these challenges, we can enhance the overall performance and adoption of VAWTs, contributing to the growth of sustainable wind energy solutions.

Author contributions. This work is performed during the PhD of MSH under the supervision of DTG as part of an Advanced Re- search Projects Agency–Energy (ARPA-E)-funded project named A Low-cost Floating Offshore Vertical Axis Wind System. MSH and DTG contributed to the analysis and interpretation of the data, and the manuscript was prepared by MSH with the help of DTG.

Competing interests. The contact author has declared that neither they nor their co-author has any competing interests.

Acknowledgements. The research presented herein was funded by the US Department of Energy Advanced Research Projects Agency-Energy (ARPA-E) under the ATLANTIS program with the project title "A Low-cost Floating Offshore Vertical Axis Wind System" associated with award no. DE-AR0001179. Any opinions, findings, and conclusions or recommendations expressed in this material are those of the authors and do not necessarily reflect the views of ARPA-E. The authors are grateful for the support of the ARPA-E program and staff, as well as the project team.

References

Ahsan, F., Griffith, D. T., and Gao, J.: Modal dynamics and flutter analysis of floating offshore vertical axis wind turbines, Renewable Energy, 185, 1284–1300, 2022.

Ancellin, M. and Dias, F.: Capytaine: a Python-based linear potential flow solver, Journal of Open Source Software, 4, 1341, 2019.

Carmo, L., Bergua, R., Wang, L., and Robertson, A.: Validation of Local Structural Loads Computed by OpenFAST Against Measurements From the FOCAL Experimental Campaign, in: International Conference on Offshore Mechanics and Arctic Engineering, vol. 87851, p. V007T09A048, American Society of Mechanical Engineers, 2024.

Cole, A., Fowler, M., Zangeneh, R., and Viselli, A.: Development of a New Federally Funded Wind/Wave/Towing Basin to Support the Offshore Renewable Energy Industry, in: SNAME American Towing Tank Conference, p. D011S003R006, SNAME, 2017.

Coquilla, R. V., Obermeier, J., and White, B. R.: Calibration procedures and uncertainty in wind power anemometers, Wind Engineering, 31, 303–316, 2007.

Fowler, M. J. L.: Floating Offshore-wind and Controls Advanced Laboratory Program: 1: 70-scale Testing of a 15 Mw Floating Wind Turbine, The University of Maine, 2023.

Gao, J., Griffith, D. T., Sakib, M. S., and Boo, S. Y.: A semi-coupled aero-servo-hydro numerical model for floating vertical axis wind turbines operating on TLPs, Renewable Energy, 181, 692–713, 2022.

Germanischer, L.: DNV Standard GL. IV - Rules and Guideline Industrial Services, Guideline for the certification of offshore wind turbines. Hamburg, www.gl-group.com/GLRenewables, 2010.

Goude, A. and Rossander, M.: Force measurements on a VAWT blade in parked conditions, Energies, 10, 1954, 2017.

Hossain, M. S., Mendoza, A. S. E., Ahsan, F., Griffith, D. T., Brownstein, I., Strom, B., and Frye, A.: Design of a Floating Vertical Axis Wind Turbine for Wind-Wave Basin Experiments, in: Journal of Physics: Conference Series, vol. 2767, p. 062007, IOP Publishing, 2024.

Kuang, L., Su, J., Chen, Y., Han, Z., Zhou, D., Zhao, Y., Jiang, Z., and Bao, Y.: Flow characteristics and dynamic responses of a parked straight-bladed vertical axis wind turbine, Energy Science & Engineering, 7, 1767–1783, 2019.

Le Fouest, S. and Mulleners, K.: The dynamic stall dilemma for vertical-axis wind turbines, Renewable Energy, 198, 505–520, 2022.

Lee, C. and Newman, J.: Wamit® user manual, versions 6.3, 6.3 PC, 6.3 s, 6.3 S-pc. Chestnut Hill, MA: WAMIT, 2006.

Lu, W.: Aerodynamic Modelling of Vertical Axis Wind Turbine Struts: Using the Lifting Line Method CACTUS, T.U.Delft Thesis, 2020.

Matha, D., Cruz, J., Masciola, M., Bachynski, E. E., Atcheson, M., Goupee, A. J., Gueydon, S. M., and Robertson, A. N.: Modelling of Floating Offshore Wind Technologies, Floating Offshore Wind Energy: The Next Generation of Wind Energy, pp. 133–240, 2016.

Murray, J. and Barone, M.: The development of cactus, a wind and marine turbine performance simulation code, in: 49th AIAA Aerospace Sciences Meeting including the New Horizons Forum and Aerospace Exposition, p. 147, 2011.

Ottermo, F., Eriksson, S., and Bernhoff, H.: Parking Strategies for Vertical Axis Wind Turbines, ISRN Renewable Energy, 2012, 1–5, https://doi.org/10.5402/2012/904269, 2012.

Parker, A.: Development and Testing of a 1: 70 Scale Model Wind Turbine of the IEA Reference 15 MW Floating Offshore System, The University of Maine, 2022.

Paulsen, U. S., Madsen, H. A., Hattel, J. H., Baran, I., and Nielsen, P. H.: Design optimization of a 5 MW floating offshore vertical-axis wind turbine, Energy Procedia, 35, 22–32, 2013.

Rezaeiha, A., Montazeri, H., and Blocken, B.: Towards optimal aerodynamic design of vertical axis wind turbines: Impact of solidity and number of blades, Energy, 165, 1129–1148, 2018.

Robertson, A.: FOCAL Campaign IV: Integrated System Control: Turbine+ Hull, Tech. rep., Pacific Northwest National Lab.(PNNL), Richland, WA (United States, 2023.

Sakib, M. S. and Griffith, D. T.: Parked and Operating Load Analysis in the Aerodynamic Design of Multi-megawatt-scale Floating Vertical-axis Wind Turbines, Wind Energy Science, 7, 677–696, https://doi.org/10.5194/wes-7-677-2022, 2022.

Shelley, S. A., Boo, S., Kim, D., and Luyties, W. H.: Comparing levelized cost of energy for a 200 mw floating wind farm using vertical and horizontal axis turbines in the northeast usa, in: Offshore Technology Conference, p. D031S040R007, OTC, 2018.

Sirnivas, S., Musial, W., Bailey, B., and Filippelli, M.: Assessment of offshore wind system design, safety, and operation standards, Tech. rep., National Renewable Energy Lab.(NREL), Golden, CO (United States), 2014.

Strickland, J., Webster, B., and Nguyen, T.: Vortex model of the Darrieus turbine: an analytical and experimental study, NASA STI/Recon Technical Report N, 80, 25 887, 1980.